



ISSN: 0976-3376

Available Online at <http://www.journalajst.com>

ASIAN JOURNAL OF  
SCIENCE AND TECHNOLOGY

Asian Journal of Science and Technology  
Vol. 16, Issue, 01, pp. 13362-13371, January, 2025

## RESEARCH ARTICLE

# THERMAL AND STRUCTURAL EVALUATION OF PHYSICALLY MODIFIED STARCH FROM LOQUAT SEEDS (*Eriobotrya japonica* Lindl.)

Stéphanie Schiavo Romko<sup>1</sup>, Camila Delinski Bet<sup>1</sup>, Daniele Bach<sup>1</sup>, RadlaZabian Bassetto Bisinella<sup>1</sup> and Egon Schnitzler<sup>1\*</sup>

State University of Ponta Grossa (UEPG), Av. Carlos Cavalcanti, 4748 - Uvaranas, ZIP 84030-900, Ponta Grossa, PR, Brazil

### ARTICLE INFO

#### Article History:

Received 11<sup>th</sup> November, 2024

Received in revised form

16<sup>th</sup> December, 2024

Accepted 29<sup>th</sup> December, 2024

Published online 22<sup>nd</sup> January, 2025

#### Keywords:

Cavitation, Thermal analysis, Loquat, Ultrasound.

### ABSTRACT

Loquat seed starch (*Eriobotrya japonica* Lindl.) was isolated, characterized, and subjected to physical modifications using ultrasound techniques at amplitudes of 40%, 50%, 60%, and 70%. Proximate analysis of the native starch revealed the following composition: moisture content (5.48%), lipid content (0.19%), protein content (3.56%), dietary fiber content (4.51%), crude fiber content (1.37%), and carbohydrate content by difference (84.77%). Thermogravimetric analysis (TG/DTG) identified three main mass loss events for all samples. The lowest onset temperature of degradation was observed in the native starch, recording 156.40°C, whereas the highest temperature was 235.18°C for the US40% sample. Changes in the L, a, and b\* color parameters were observed between native and ultrasound-modified samples. A decrease in both the initial and peak gelatinization temperatures was noted for sonicated samples. Native loquat seed starch exhibited a reduction in pasting temperature as the ultrasonic vibration amplitude increased. Peak viscosity showed a more pronounced increase up to 50% treatment, then gradually decreased when reaching 70% amplitude. Isolated starch granules were examined using polarized light microscopy and scanning electron microscopy, which revealed a mixture of irregular, truncated, and spherical granules. The molecular structure of the starch remained unchanged regardless of the treatment method applied, as confirmed by unaltered functional groups in the FT-IR spectra. However, the intensity of the characteristic peaks was affected by the different treatments. Starch is an excellent source of biodegradable material derived from plant sources, which is environmentally friendly and cost-effective. Therefore, it is potentially used as an alternative to plastic in food packaging. In this context, various efforts have been made to develop biodegradable antioxidant films using loquat seed starch.

**Citation:** Stéphanie Schiavo Romko, Camila Delinski Bet, Daniele Bach, RadlaZabian Bassetto Bisinella and Egon Schnitzler. 2025. "Thermal and Structural Evaluation of Physically Modified Starch from Loquat Seeds (*Eriobotrya Japonica* Lindl.)." *Asian Journal of Science and Technology*, 16, (01), 13362-13371.

Copyright©2025, Stéphanie Schiavo Romko et al. This is an open access article distributed under the Creative Commons Attribution License, which permits unrestricted use, distribution, and reproduction in any medium, provided the original work is properly cited.

## INTRODUCTION

*Eriobotrya japonica* Lindl., commonly known as loquat, is a fruit of the Rosaceae family and originates from Japan. It features a yellow color, velvety skin, and a sweet, slightly acidic pulp. The skin is rich in bioactive compounds, and the fruit can contain up to five brown seeds inside (ZHU *et al.*, 2021; LI *et al.*, 2023; WU *et al.*, 2022). Loquat seeds account for approximately 30% of the fruit's fresh weight (CHEN *et al.*, 2020; CAO & SONG, 2019) and are often discarded despite containing the highest starch content in the loquat fruit (THORY & SANDHU, 2017; LIU *et al.*, 2023). Starch is widely used in both food and non-food industries due to its low cost and abundant availability. However, the morphology, structure, and properties of starch vary significantly among plant sources, influencing its usability in diverse applications (GUO *et al.*, 2022; MARTINEZ *et al.*, 2023). With the advancement of food and non-food industries, there is an increasing interest in exploring new starch sources with innovative and functional properties suitable for a wide range of industrial contexts.

According to Brazilian legislation (RDC No. 263 of September 2005), starch is defined as:

"[...] the starchy product extracted from edible parts of cereals, tubers, roots, or rhizomes, which may undergo processes such as soaking, grinding, extraction, heat treatment, and/or other safe technological processes for food production" (ANVISA, 2005).

Due to its versatility, starch acts as a stabilizer, gelling agent, thickener, moisture retainer, and viscosity and volume agent in food products (COLMAN *et al.*, 2021). To enhance the physical, chemical, and functional characteristics of native starch for specific industrial applications, starch undergoes modifications that may be physical, chemical, enzymatic, or combined (dual modification) (PUNIA *et al.*, 2020; KHAN *et al.*, 2022). Among these techniques, ultrasound-assisted physical modification has gained prominence in the food industry due to its advantages, such as increased yield and purity, reduced processing time, and the absence of chemicals (SCHMIELE *et al.*, 2021; ZHANG *et al.*, 2023). Starch modifications enable the enhancement of specific functionalities, including texture, clarity, cooking properties, retrogradation, reduced syneresis, gelling, and thermal stability (ASHOGBON, 2021). Therefore, this study aims to evaluate the effects of ultrasound application on *Eriobotrya japonica* starch using thermal, morphological, structural, and pasting profile analyses.

\*Corresponding author: Egon Schnitzler

State University of Ponta Grossa (UEPG), Av. Carlos Cavalcanti, 4748 - Uvaranas, ZIP 84030-900, Ponta Grossa, PR, Brazil

## MATERIALS AND METHODS

The loquat seeds used were extracted from ripe fruits obtained from wild cultivar trees located in the city of Caetano Mendes, Paraná, Brazil, at a latitude of 24°37'35"S and a longitude of 50°38'24"W.

**Starch extraction:** The starchy material was extracted in an aqueous medium without the use of chemicals, following an adapted methodology based on Bet *et al.* (2018) and Bet *et al.* (2021). Initially, the seeds were removed from the fruit and dried in a forced-air oven at 45°C for 48 hours. Once dried, the seeds were separated from the spicules and ground using an industrial blender. The starch extraction involved mixing the ground seeds with distilled water in a 1:4 ratio (w/w) and stirring for 10 minutes. The resulting suspension was filtered sequentially through 150-mesh and 270-mesh sieves, then allowed to settle under refrigeration for 24 hours. Afterward, the sediment was dried again in a forced-air oven at 40°C for 24 hours. The dried starch was subsequently ground, standardized through sieving, stored in airtight containers, and placed in a desiccator until further analysis.

**Physical modification:** The starch granules were modified using ultrasound, performed with the assistance of a USC 1400 device operating at a constant frequency of 20 kHz and a generator output power of 750 W. Ultrasound waves were applied to suspensions of starch and deionized water (10% w/v), which were kept in an ice bath to control the heating of the starch during the process. The sample treatment was set for 30 minutes, with amplitudes of 40%, 50%, 60%, and 70%, and a controlled temperature of 45°C to prevent starch gelatinization during modification (LIU *et al.*, 2018).

**Physicochemical Analyses:** The proximate analysis was conducted following the official AOAC methods for proteins (920.87), lipids (968.20), ash (923.03), moisture (934.01), and dietary fiber (994.43). The carbohydrate content was calculated by difference.

**Fourier-transform infrared spectroscopy (FTIR):** The Fourier-transform infrared (FTIR) spectrometer used was the IRPrestige21 model from Shimadzu Corp., Kyoto, Japan, where the samples were characterized. For the analysis, pellets were prepared using 2 mg of the sample (dry basis) and 100 mg of dry KBr. The spectra were recorded at a resolution of 4 cm<sup>-1</sup> with an average of 64 scans in the range of 4000-400 cm<sup>-1</sup> (DUPUIS, 2017).

**Viscoamylography (RVA):** To obtain the pasting profile of the samples using a viscoamylograph, model RVA-4 (Newport, Australia), the methodology proposed by Ito *et al.* (2018) was employed with some modifications. The moisture content of the samples was determined using an infrared moisture analyzer balance (Sartorius MA 35M-000230V1, AR, Germany), at a temperature of 105°C for 15 minutes. Suspensions of 8% (w/w) dry basis were mixed with deionized water to achieve a final mass of 28 g. To determine the amount of starch needed to mix with the deionized water, Equation 3 was used, which requires 2.24 g of dry basis sample:

$$X = \frac{224}{100-U} \quad (1)$$

Where: x = mass of starch to be measured (g); U = moisture content of the native starch.

The controlled heating and cooling system was performed under constant agitation, maintaining 50°C for 2 minutes, heating from 50°C to 95°C at 6°C per minute, holding at 95°C for 5 minutes, cooling back to 50°C at 6°C per minute, and finally maintaining 50°C for 2 minutes.

**Colour analysis:** A previously calibrated colorimeter (MiniScan EZ 4500L Reston, USA) was used to measure the colour parameters of the samples: brightness (L\*, where 0 = black and 100 = white) and a\*

and b\* chromaticity values (where -a\* = green and +a\* = red; -b\* = blue and +b\* = yellow) (FALADE, OMIWALE, 2015).

**Thermal analysis:** The thermogravimetric curves were obtained in thermobalance (TGA-50, Shimadzu, Japan). A mass of approximately 8 mg was weighed in an alpha alumina crucible and subjected to controlled heating (30 - 650 °C) under airflow of 150 mL min<sup>-1</sup>, at a heating rate of 10 °C min<sup>-1</sup>. The curves that correspond to the first derivative of the TG curve (DTG) and the percentages of mass loss were obtained using the data analysis software TA-60 WS (BET, 2021). To evaluate the starch gelatinization process, differential scanning calorimetry (DSC) was used. A starch suspension (1:4, w/v) was prepared in aluminium crucibles, sealed, and kept at room temperature for 1 h before analysis, to balance the moisture content. The sample was then heated from 30 to 100 °C under airflow (50 mL min<sup>-1</sup>) and heating rate of 5 °C min<sup>-1</sup>. The DSC Q-200 equipment (T.A. Instr. Ltd., USA) was used, previously calibrated and verified with the Indium standard (99.99% purity) according to the manufacturer's specifications. To obtain and interpret the curves, the Universal Analysis software (OLIVEIRA *et al.*, 2014) was used.

**Field emission gun-Scanning electron microscopy (FEG-SEM):** The size and shape of the taro starch granules were evaluated using the field scanning electron microscope (MIRA 3 Tescan, Czech Republic). A metallisation (120 s; 40 mA) of the samples with gold before the analysis was necessary to promote the passage of electrons in the samples that were placed on a carbon tape. The parameters were: 15 kV of voltage in the field emission gun generated by a lamp with tungsten filament (ITO *et al.*, 2018; KUBIANKI *et al.*, 2018).

**X-ray powder diffractometry (XRD):** The following parameters were used to obtain the relative crystallinity patterns of starch samples: CuK $\alpha$  radiation ( $\lambda = 1.544 \text{ \AA}$ ), configured at a voltage of 40 kV, and a current of 20 mA, scan time of 0.5° min<sup>-1</sup> and Bragg-Brentano geometry of 3° <  $\theta$  < 50° (2 $\theta$ ). The instrument was an X-ray diffractometer (Ultima IV; Rigaku, Japan). The relative crystallinity (RC) was calculated quantitatively according to the literature (COLMAN *et al.*, 2014) using the Origin software (Microcal Inc., Northampton, MA, version 6.0) according to Eq. 2:

$$RC = \frac{A_p}{A_p + A_b} \times 100 \quad (2)$$

Where: RC = relative crystallinity; A<sub>p</sub> = peak area; A<sub>b</sub> = basis area, which refers to the amorphous area of the diffractograms.

**Statistical analysis:** Following the normality of the data, the Levene test was used to evaluate the homoscedasticity of variances (p > 0.05). Analysis of variance (ANOVA) was applied to check the differences between the samples, then Tukey's test ( $\alpha = 0.05$ ) was performed to compare the means. The program used was Action Stat (version 3.3.2, Statcamp, Brazil).

## RESULTS AND DISCUSSION

**Physicochemical analyses:** The physicochemical analyses for characterizing the proximate composition of native loquat seed starch are presented in Table 1. The native starch sample showed a moisture content below 15% (5.48%) and an ash content below 1.4% (1.37%), in accordance with Brazilian legislation for commercial starches (ANVISA, 2005). The protein content (3.56%) is slightly higher than that reported in the literature (BARBI *et al.*, 2018; LOPES *et al.*, 2018). These differences may be due to variations in cultivars and different starch extraction methods. The lipid content of the native loquat seed starch sample (0.19%) is somewhat similar to values reported for other seed starches in the literature, such as corn starch (0.51%) (YUAN *et al.*, 1993). Another study reported a lipid content of 0.34% for loquat seed starch (COSTA *et al.*, 2022). According to the literature on starches, lower levels of protein, ash, lipids, and fiber generally indicate higher starch quality and purity (HOOVER, 2001).

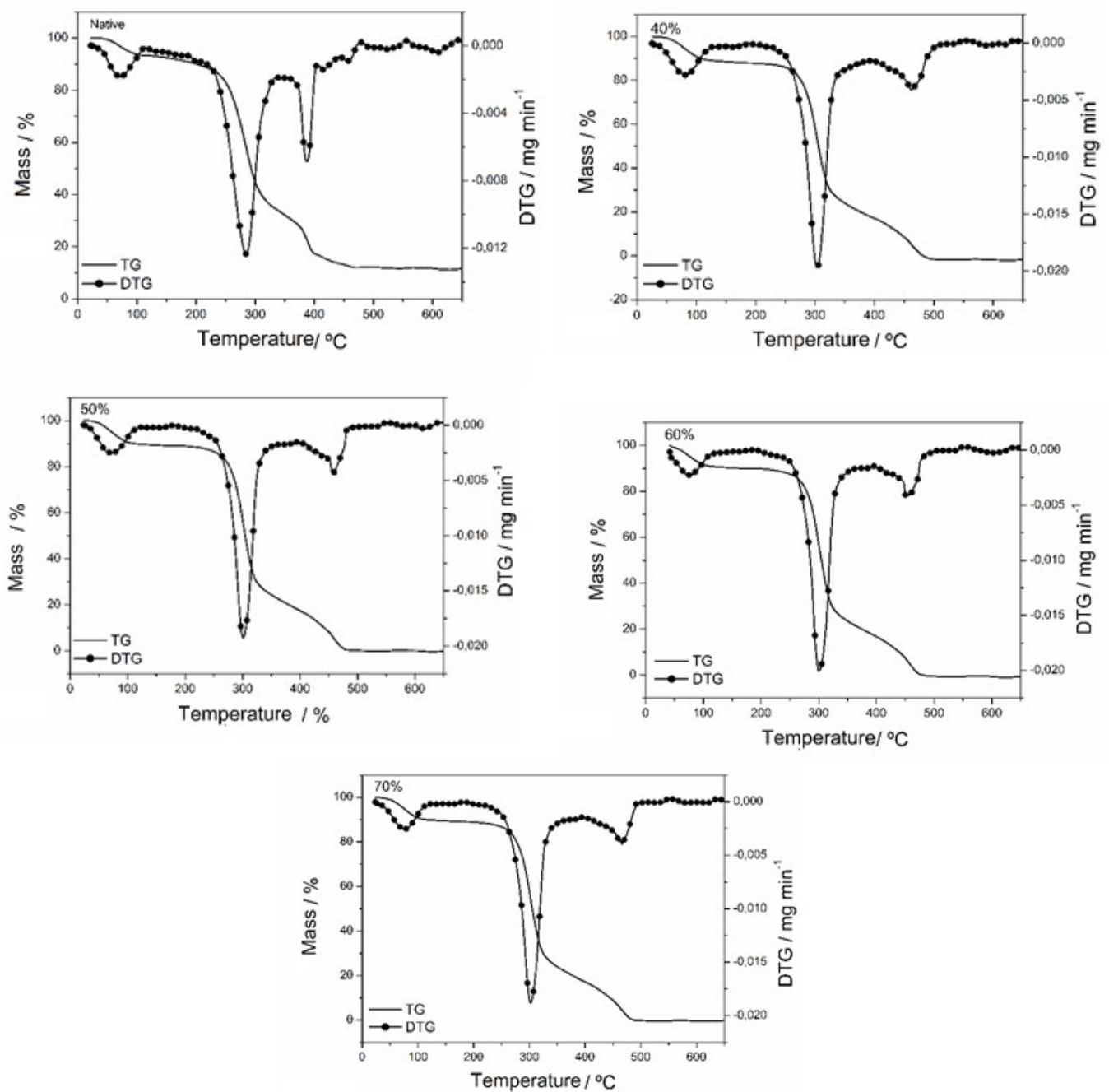
**Table 1. Proximal composition of native loquat starch**

Sample	Moisture (%)	Ash (%)	Protein (%)	Lipids (%)	Dietary fiber (%)	Carbohydrates by difference (%)
Native Starch	5.48 ± 0.1	1.37 ± 0.02	3.56 ± 0.09	0.19 ± 0.007	4.51 ± 0.13	84.77 ± 0.35

Source: The author (2023).

**Table 2. Color parameters of the starches**

Starches	L	a*	b*
Native	65.07±0.14 <sup>bc</sup>	9.59±0.05 <sup>a</sup>	20.75±0.19 <sup>a</sup>
40%	66.85±0.23 <sup>a</sup>	8.65±0.02 <sup>b</sup>	18.71±0.03 <sup>c</sup>
50%	65.30±0.17 <sup>b</sup>	8.50±0.06 <sup>b</sup>	17.86±0.17 <sup>c</sup>
60%	62.61±0.19 <sup>d</sup>	7.99±0.08 <sup>c</sup>	16.89±0.30 <sup>d</sup>
70%	64.46±0.18 <sup>c</sup>	7.99±0.09 <sup>c</sup>	16.86±0.19 <sup>d</sup>
p-value	<0.001	<0.001	<0.001

<sup>abcd</sup> Different letters in the same column represent significant differences according to the Tukey Test (p<0.05).**Figure 1. TG curves for native and modified loquat starch US 40%, US 50%, US 60%, and US 70%**

**Colour Analysis:** The color system established by the International Commission on Illumination (CIE) offers a precise definition of the color space. Within this system, color perception is based on three essential components: luminosity or brightness, hue or color tone, and saturation or chromatic intensity. The underlying theory assumes that humans possess three types of color receptors (cones) that are specifically sensitive to red, green, and blue. By combining these primary colors, all other shades are generated. The colorimetric parameters of native and modified starches are shown in Table 2. The L value (luminosity) of loquat seed starches varied significantly ( $p < 0.05$ ) from 66.96 to 62.71, showing a decrease in L value for starches modified with ultrasound at 60% and 70% amplitudes. Other research reported a higher L\* value (79.23) due to its extraction in a neutral pH (COSTA *et al.*, 2022). The cavitation induced by ultrasound treatment causes the collapse of bubbles, resulting in high-speed collisions between particles and the impact of liquid jets on the starch granule surface. This phenomenon may be responsible for the passage of pigments, impurities, or even antioxidant compounds through fissures in the starch granule structure. This process enables the binding of starch molecules and, as a consequence, reduces the whiteness of the material. According to the literature, color is an important quality characteristic of starch (SIT *et al.*, 2014). The study results showed that ultrasound modification had a significant impact on the a and b values of the samples, resulting in a decrease in red ( $a^*$ ) and a decrease in yellow ( $b^*$ ) compared to native starch. This effect of reducing starch color intensity after ultrasound modification has also been corroborated in previous research (KRISHNAKUMAR, SAJEEV, 2017; BERNARDO *et al.*, 2018). A lower shift towards yellow was associated with a lower protein content, resulting in a decreased b chromaticity value (ZHANG *et al.*, 2005). Other researchers observed an increase in yellow hue (b) in water yam starch, attributed to the release of pigments during the breakdown of the cellular structure, which then passed through the sieve used to isolate the starch (BERNARDO *et al.*, 2018). A similar observation was suggested in a study on ultrasound-extracted taro starch (SIT *et al.*, 2014).

#### **Thermogravimetry and Derivative Thermogravimetry (TG/DTG):**

The method of subjecting starch to different temperature ranges, both high and low, is widely employed in the food industry and in the manufacturing of starch-based materials. During food processing, thermal degradation and monitoring the stability of starch-containing materials are crucial factors. This approach facilitates the understanding of degradation mechanisms and the tracking of starch structure behavior during thermal treatment (LIU *et al.*, 2018). The thermogravimetric technique has been applied to investigate the thermal stability and decomposition of polymers. When used in conjunction with other analyses, thermogravimetry can provide more accurate information for understanding the thermal properties of both native and modified starches (SOWIŃSKA-BARANOWSKA; MACIEJEWSKA, 2022). Loquat seed starch exhibited three mass loss stages, similar to amaranth starch (BET, 2021). The thermogravimetric curves obtained for loquat seed starch are shown in Figure 1. As observed in the thermogravimetric curves, the loquat seed starch samples exhibited three mass loss stages. The first stage was related to moisture loss, ranging between 6.70-11.21%, as shown in Table 4. The moisture content of the starch was lower than that found by Costa *et al.* (2022) in their study of loquat seed starch. The second stage involved the depolymerization of amylose and amylopectin, as well as starch degradation, followed by the oxidation of the sample until ash formation. Other researchers observed that the second stage of mass loss involves the depolymerization of amylose and amylopectin chains, with amylose showing an endothermic melting temperature range between 140°C and 180°C (BET, 2021). Thermogravimetric Derivative (DTG) curves are useful for distinguishing mass loss events, as they indicate the decomposition rate relative to temperature (ANDRADE *et al.*, 2020). The loquat seed starches exhibited three main mass loss events. The first loss occurred between 30°C and 136.27°C. The temperature peak calculated by DTG during this first event ranged from 72.0°C to 82.37°C, followed by a period of stability, varying from 115.81°C to 235.18°C.

The largest range was observed in the US40% sample (137.13°C – 235.18°C) compared to native starch. Decomposition and oxidation of organic matter occurred in consecutive stages during the second and third mass losses (OLIVEIRA *et al.*, 2014). The lowest onset degradation temperature was observed in native starch, registering 156.40°C, while the highest was 235.18°C for the US40% sample. Ultrasound treatment has the capacity to break down starch chains, with longer and more linear chains being affected more rapidly than smaller molecules. This happens because larger molecules have longer relaxation times, making them more susceptible to ultrasound action. These changes in thermal behavior may be associated with the collapse of high-intensity bubbles in the liquid medium, releasing a significant amount of energy. This process results in the formation of hotspots in the suspension, which play a crucial role in breaking down or destructuring starch molecules. Consequently, there is a loss of alignment between amylose and amylopectin, allowing starch molecules dispersed in the liquid medium to bond with different attractive forces (CUI; ZHU, 2020). The depolymerization process of starches typically begins above 300°C and can be confirmed by the temperature peak ( $T_p$ ) recorded by DTG during the second mass loss (OLIVEIRA *et al.*, 2014). The modified samples showed a higher temperature compared to the native starch sample, which exhibited the lowest initial temperature ( $T_i$ ) of 387.65°C. The ash content of the samples was 3.03% (native), 2.38% (US40%), 2.95% (US50%), 2.59% (US60%), and 2.71% (US70%), respectively, which is related to the amount of minerals that remain after aqueous extraction.

**Differential scanning calorimetry (DSC):** Heating starch granules in the presence of water causes swelling due to the disruption of the crystalline structure and the formation of hydrogen bonds between water molecules and the hydroxyl groups of amylose and amylopectin (ZOBEL *et al.*, 2021). This process results in changes in starch composition, leading to the destabilization of the granules' internal crystalline structure when the temperature reaches a specific range, as observed in studies by Odeniyi *et al.* (2023), Wang *et al.* (2022), and Kaur *et al.* (2021). This phenomenon, known as gelatinization, can be assessed using Differential Scanning Calorimetry (DSC), represented by the endothermic event exhibited by all samples, as shown in Figure 2.

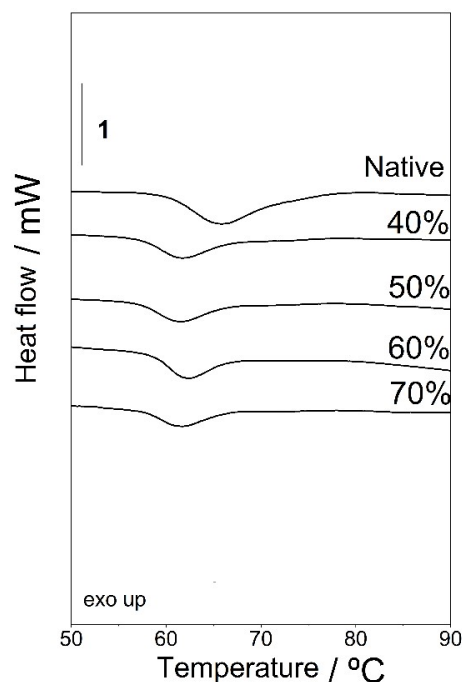


**Figure 2.** DSC curves of native and ultrasound-modified starch US 40%, US 50%, US 60%, and US 70%

The application of ultrasound to starch granules has shown significant impacts on morphological and physicochemical properties, as observed by Amini *et al.* (2015).

A leftward shift in the onset of the gelatinization curve was observed, suggesting a decrease in the initial temperature of the process. The narrowing of the peak associated with ultrasound treatment may indicate that sonication distorted the amorphous and disorganized regions of the starch granule, thereby increasing the homogeneity of the material (AMINI *et al.*, 2015). More recent studies support these findings, highlighting that ultrasound application can enhance gelatinization efficiency and promote structural reorganization of the granules (ZHOU *et al.*, 2023; MA *et al.*, 2022). In the present work, the results regarding the gelatinization of both native and modified loquat starch are presented in Table 4. It was observed that the modified starch exhibited higher gelatinization efficiency, attributed to the increased homogeneity of the granules after ultrasound modification. These findings are consistent with recent studies on starches from various botanical sources, where ultrasound has been shown to be an effective tool for modifying thermal and functional properties (LI *et al.*, 2021).

modified rice starch following physical treatments, further corroborating the changes in enthalpy seen in previous studies. Additionally, a statistical similarity ( $p < 0.05$ ) was observed in the gelatinization process between the US40% and US50% samples, with peak temperatures ( $T_p$ ) being nearly identical, ranging from 61.46 to 61.38°C. These values were lower than those typically reported in the literature for traditional starch sources, such as corn starch ( $T_p$ —73.2°C) and cassava starch ( $T_p$ —69.0°C), and also lower than for non-traditional starches like amaranth, as mentioned in recent studies (WANG *et al.*, 2022). Intensive ultrasound parameters may damage starch granules, potentially altering their crystallinity. The cavitation induced by ultrasound facilitates water penetration into the starch structure, accelerating the gelatinization process and reducing the enthalpy energy associated with it (ZHANG *et al.*, 2023). No significant changes in gelatinization enthalpy ( $\Delta H_{gel}$ ) were observed between the US50% and US60% samples (Table 4), indicating that the modification was insufficient to completely disrupt some of the

**Table 4. DSC results of native and modified starches**

Samples	$T_o/^\circ\text{C}$	$T_p/^\circ\text{C}$	$T_c/^\circ\text{C}$	$\Delta H_{gel} / \text{J g}^{-1}$
Native	60.19±0.45 <sup>a</sup>	65.37±0.28 <sup>a</sup>	70.64±0.16 <sup>a</sup>	3.71±0.19 <sup>c</sup>
40%	57.27±0.16 <sup>c</sup>	61.46±0.14 <sup>c</sup>	66.59±0.06 <sup>c</sup>	4.53±0.13 <sup>a</sup>
50%	57.46±0.11 <sup>c</sup>	61.38±0.05 <sup>c</sup>	66.38±0.18 <sup>c</sup>	4.36±0.13 <sup>ab</sup>
60%	58.73±0.29 <sup>b</sup>	62.18±0.05 <sup>b</sup>	66.23±0.05 <sup>c</sup>	4.23±0.29 <sup>ab</sup>
70%	57.64±0.6 <sup>c</sup>	61.62±0.09 <sup>c</sup>	67.10±0.17 <sup>b</sup>	3.95±0.12 <sup>bc</sup>

(\*)  $T_o$  “onset” or initial temperature,  $T_p$  peak temperature,  $T_c$  “endset” or conclusion temperature,  $\Delta H_{gel}$  gelatinization enthalpy. Values followed by same letter in the same column are not significantly different by Tukey’s test ( $p < 0.05$ ).

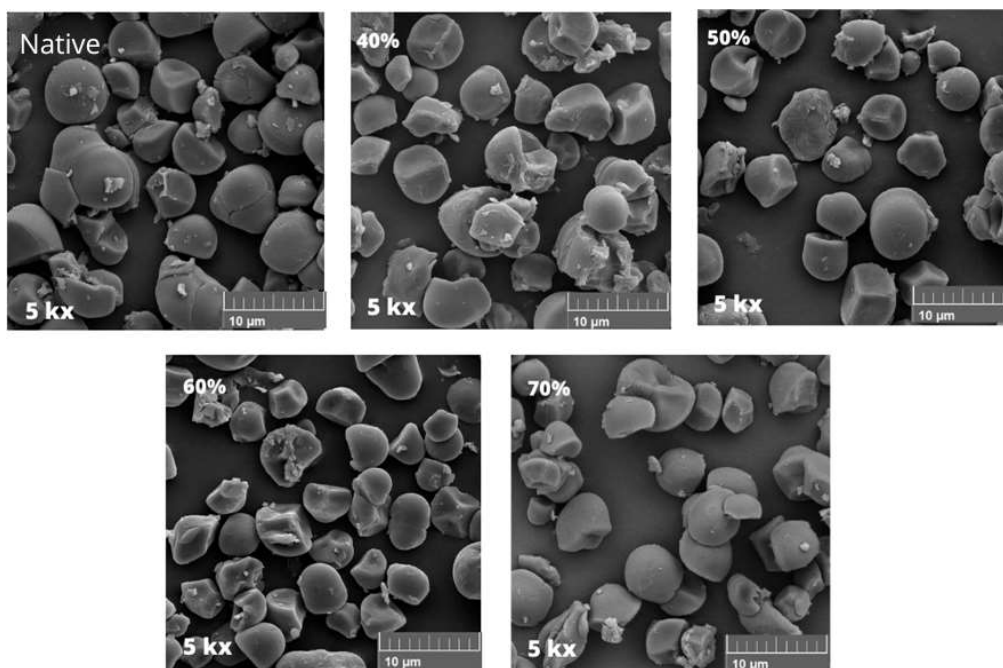


**Figure 3. Microimages of native and modified loquat seed starch US 40%, US 50%, US 60%, and US 70%**

The sample treated with 40% amplitude showed a slight decrease in the onset temperature (57.27°C) compared to the native starch. The lowest gelatinization temperature range ( $\Delta T = 7.53^\circ\text{C}$ ) was found in the starch modified with 60% amplitude ultrasound. Similarly, the lowest peak temperatures ( $T_p$ ) during the gelatinization process were observed in the sonicated samples (Table 4). The US60% sample exhibited the lowest  $T_c$  (66.23°C). These results align with recent studies, such as Zhang *et al.* (2023), which observed comparable behavior in cassava and yam starches subjected to higher ultrasound levels. This suggests that the breakdown of weaker crystals leaves behind those with greater resistance. The impact of ultrasound on starches can vary based on botanical source, medium concentration, temperature, starch composition, and equipment type, complicating the direct comparison of experimental data across different studies (WANG *et al.*, 2022). Changes in gelatinization enthalpy due to ultrasound treatment have been reported in a variety of starches. Recent work by Liu *et al.* (2021) demonstrated similar patterns in

double helices in the amorphous and crystalline regions of the granules.

**Field emission gun-scanning electron microscopy (FEG):** The isolated starches were observed using polarized light and scanning electron microscopy (Figure 3). The loquat starch granules displayed a combination of irregular, truncated, and spherical shapes, similar to those of jackfruit and longan starches, as reported by Guo *et al.* (2018). Recent studies by Li, Fan, and Hu (2023) further confirm that loquat starch granules exhibit semicircular, square, and irregular shapes, with notable variations compared to other botanical sources like amaranth, whose granules typically exhibit polyhedral or polygonal shapes (BET *et al.*, 2021). The observed differences in starch morphology, hilum position, and granule size are often attributed to the distinct botanical origins, biosynthetic pathways within the amyloplast, and unique physiological characteristics of each plant (WANG *et al.*, 2022).

The application of ultrasound (US) to starch suspensions can induce two main mechanisms: erosion and fracture. Erosion refers to the gradual detachment of particles from the surface of starch granule clusters, while fracture, also referred to as "fissuring," involves the splitting of clusters into smaller aggregates due to the propagation of cracks initiated at surface defects. The specific process that dominates depends on the energy levels applied during ultrasound treatment (ZHANG *et al.*, 2023). However, the opposite effect can also occur, where ultrasound may promote the agglomeration of starch granules, increasing their size and altering their morphology due to the formation of new bonds between liberated polymer chains (JAIN *et al.*, 2022). Ultrasound treatment typically results in the formation of visible pores and cracks on the surface of starch granules, a phenomenon widely observed in ultrasound-modified starches from various botanical sources. Studies on wheat and corn starches have shown similar structural modifications, where the surface integrity of the granules is disrupted (KAUR; GILL, 2019). Wang *et al.* (2021) observed that rice starch granules subjected to ultrasound underwent notable surface fissuring, with the extent of damage increasing proportionally to the ultrasound power applied. Despite these surface alterations, it is worth noting that granule size is not always significantly affected by the ultrasound process, with changes in size being more dependent on treatment parameters such as amplitudes and duration (WANG *et al.*, 2021).

**X-ray powder diffractometry (XRD):** The X-ray diffraction (XRD) patterns for the native and modified loquat seed starch samples are shown in Figure 4, and the percentages of relative crystallinity are presented in Table 5.

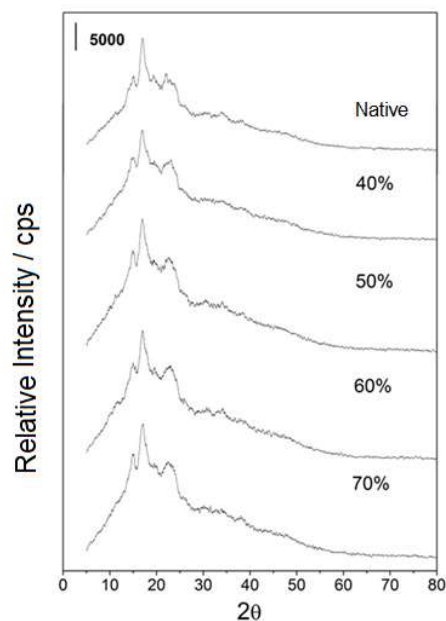


**Figure 4. X-ray diffraction (XRD) patterns for native and modified loquat starch samples US 40%, US 50%, US 60%, and US 70%.**

**Table 5. Crystallinity and peaks for the diffraction pattern**

Sample	Relative crystallinity (%)	Standard deviation
Native	27.77 <sup>a</sup>	0.001
40%	21.01 <sup>c</sup>	0.001
50%	25.02 <sup>ab</sup>	0.01
60%	25.31 <sup>b</sup>	0.001
70%	27.29 <sup>ab</sup>	0.001

<sup>abcd</sup> Different letters in the same column represent significant differences according to the Tukey Test ( $p < 0.05$ ).

The main peaks observed in the diffractograms for the loquat seed starches were at 15°, 17°, and 23°, with the peak at 17° being the most pronounced. These peaks give them a type C diffraction pattern. Similar peak values were found by Li, Fan, and Hu *et al.* (2023) at

5.6°, 15.1°, 17.1°, 17.9°, and 23°, which represented the characteristic combined peaks of type A and type B starch and indicated that loquat seed starch is a complex type C starch. These data are consistent with Costa *et al.* (2022). A mixture of type A and type B starches is produced by certain roots and seeds (SING *et al.*, 2003). Higher levels of crystallinity are interrelated with a lower amylose content, as the degree of crystallinity has been shown to be inversely proportional to the amylose content. Thus, the amylose content in starch is highly responsible for retrogradation, which has a negative effect on food compositions due to the occurrence of gelatinization at high temperatures. It was observed that the peaks remained similar after modification, which was not sufficient to cause significant changes in the peaks.

**Fourier-transform infrared spectroscopy (FTIR):** Fourier-transform infrared (FT-IR) spectroscopy is an essential technique for characterizing molecular structures by recording absorption bands in the mid-infrared region (4000–400  $\text{cm}^{-1}$ ), which enables the identification of functional groups based on their vibrational frequencies (CARPENA *et al.*, 2020). This method allows for detailed investigation of the chemical composition of starches, and it was applied to analyze loquat seed starch in this study. The transmittance spectra for both native and ultrasound (US)-modified loquat starches (US 40%, US 50%, US 60%, and US 70%) are presented in Figure 5.

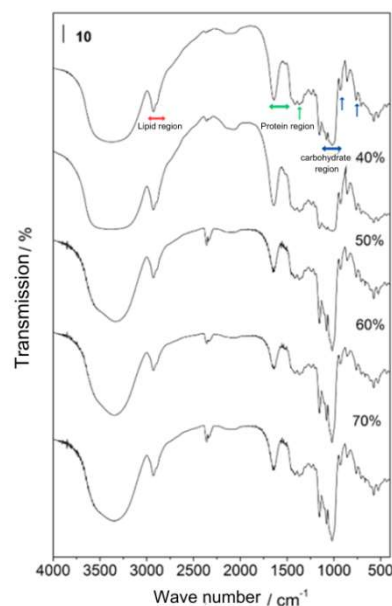


**Figure 5. Transmittance spectra for native and US-modified loquat starch US 40%, US 50%, US 60%, and US 70%.**

The FT-IR spectra were divided into three main regions for clearer interpretation: the lipid region, protein region, and carbohydrate (starch) region (GHARSALLAH *et al.*, 2021). In the native starch spectrum, broad bands in the range of 3400–3200  $\text{cm}^{-1}$  were detected, corresponding to O–H stretching vibrations, which are commonly found in starch and were present in all modified samples. Occasionally, this band may show a triangular shape due to the overlap with asymmetric N–H stretching vibrations (GONÇALVES *et al.*, 2019). Additionally, absorption in the region between 2700 and 3300  $\text{cm}^{-1}$ , associated with the asymmetric stretching of C–H bonds, is attributed to the presence of lipids in the starch matrix, as also observed in similar studies (ZHAO *et al.*, 2020). Characteristic protein-related bands were found around 1700  $\text{cm}^{-1}$  (amide I) and 1450  $\text{cm}^{-1}$  (amide II), corresponding to peptide C=O stretching and N–H bending vibrations, respectively (ALAMRI *et al.*, 2021). These amide bands are related to the conformational structure of proteins within the starch granules, with amide I specifically indicating protein secondary structure (RAMOS-GUZMÁN *et al.*, 2023). The presence of these bands suggests minimal protein contamination within the starch sample, which is common in starches extracted from seeds.

The absorption bands around  $1100\text{ cm}^{-1}$  correspond to C–O and C–C stretching, along with C–O–H bending vibrations, which are characteristic of the polysaccharide backbone of starch (WANG *et al.*, 2023). The bands in the region of  $1000\text{--}1100\text{ cm}^{-1}$ , particularly those near  $1000\text{ cm}^{-1}$ , can be associated with the amorphous regions of the starch structure, as these correspond to C–O–C glycosidic bond vibrations and ring vibrations (NURHADI *et al.*, 2022). Similar bands were observed in previous studies of modified starches from various botanical sources (ZHAO *et al.*, 2020).

Despite the different ultrasound treatments applied, the molecular structure of the loquat starch granules remained unchanged, as indicated by the preservation of the main functional groups in the FT-IR spectra. However, changes in the intensity of characteristic peaks suggest that the treatments did affect the molecular ordering and interaction between components within the starch granules. For instance, regions below  $1000\text{ cm}^{-1}$ , which are considered the fingerprint region of starch molecules, showed peaks corresponding to C–O–C linkages that align with amylose and amylopectin structures (KODAMA *et al.*, 2023). Overall, the FT-IR analysis confirmed that the ultrasound treatments did not significantly alter the primary molecular structure of the starch, although they did induce subtle changes in peak intensities, reflecting modifications in granule morphology and molecular interactions.

**Viscoamylography (RVA):** The Rapid Visco Analyzer (RVA) is a vital tool for evaluating the pasting properties of starch by controlling the heating and cooling cycles of a starch-water suspension while applying a constant shear force. The RVA profile reveals how temperature, mechanical agitation, and time influence the viscosity behavior of starch paste, offering valuable insights into key processes such as gelatinization, granule swelling, leaching of starch components (primarily amylose), and granule rupture. Additionally, it provides information on starch retrogradation, a process where starch molecules reassociate, leading to a reduction in molecular distance and the formation of a gel-like structure upon cooling (RHA *et al.*, 2017). It can be observed that the pastes exhibited a shiny appearance and that the starch modified at 50% showed a more viscous texture compared to the paste modified at 70%, which appeared more fluid. This can be confirmed by the RVA curves shown in Figure 7. The modified loquat starch exhibited an increase in paste viscosity across all treatments, with the most significant enhancement noted at a 50% vibration amplitude. However, a reduction in viscosity was observed with higher amplitudes. This decrease in viscosity can be attributed to the breakdown of long starch chains, which diminishes the interaction strength between particles (WANG *et al.*, 2023). Additionally, Zhao *et al.* (2023) suggest that a reduction in starch granule size may lead to decreased water retention capacity, impacting the overall viscosity of the starch paste. The data extracted from the RVA curves is presented in Table 6.

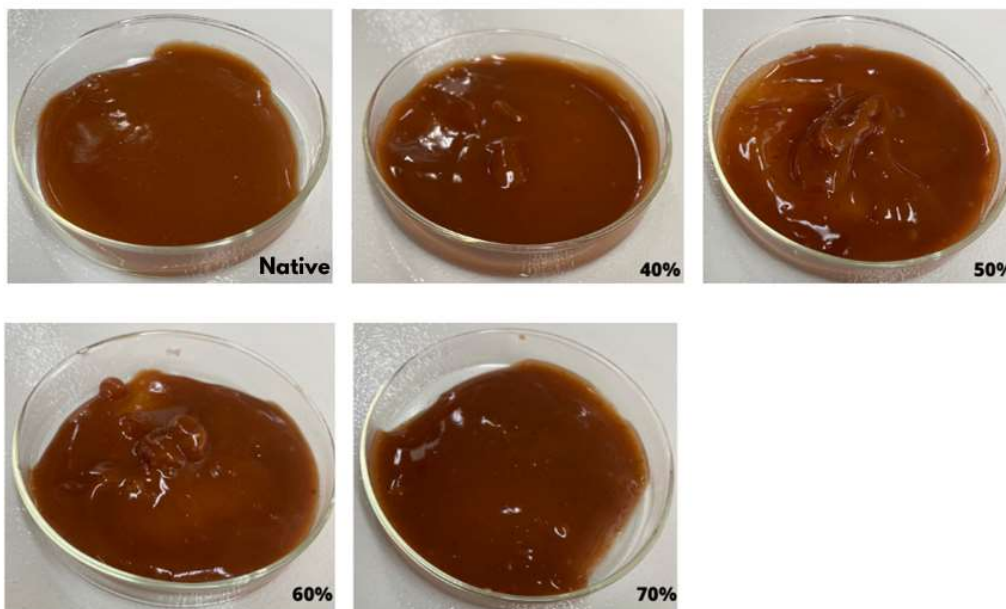


Figure 6. Native and US-modified loquat starch pastes

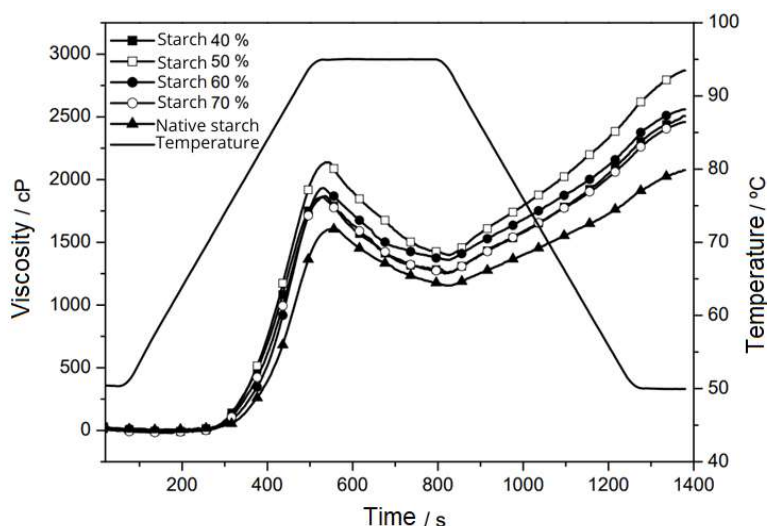


Figure 7. RVA curves for native and US-modified loquat starch

**Table 6. Data on the viscosity of native and modified loquat starch**

Samples	Tp (°C)	Vp (mPa.s)	Vm (mPa.s)	Breakdown (mPa.s)	Vf (mPa.s)	Retrogradation (mPa.s)	Tp (s)
Native	78.70	1605	1155	450	2705	920	547.80
40%	74.85	1868	1260	608	2606	1246	535.80
50%	74.90	2137	1398	739	2869	1471	535.80
60%	76.40	1933	1360	573	2559	1199	532.20
70%	74.00	1859	1251	608	2458	1207	528.00

Tp: paste temperature (°C); Vp: peak viscosity; Vm: average viscosity; Vf: final viscosity; Tp: peak temperature. mPa·s = millipascal-seconds, s = seconds.

Notably, native loquat starch demonstrated a decrease in paste temperature with increasing ultrasound vibration amplitude. Peak viscosity exhibited a marked increase up to the 50% treatment, followed by a gradual decline at the 70% amplitude. This trend indicates that higher peak viscosities are associated with more significant starch breakdown, although the minimum viscosity during shear remained higher than that of native starch. The tendency for retrogradation was also found to increase more substantially with higher peak viscosity, while its intensity diminished at higher vibration amplitudes due to lower viscosity levels. Consequently, the final viscosity reflected this trend, being higher than that of native starch only in the 40% and 50% treatments. In contrast, starches treated at 60% and 70% exhibited lower final viscosity values compared to the native starch. Importantly, the time required to reach maximum viscosity was shorter for all treatments relative to the native starch. This is consistent with findings from ultrasound-treated rice starch, where an increase in peak viscosity and a reduction in peak time and paste temperature were observed (LI et al., 2023). The authors emphasized that the viscosity profile following ultrasound modification is influenced by the specific type of starch employed.

## CONCLUSION

The detailed analysis of native and ultrasound-modified loquat seed starch provided comprehensive insights into its physicochemical and rheological properties. Ultrasound modifications led to significant changes, including alterations in color, degradation and gelatinization temperatures, and starch rheological properties. Infrared spectroscopy confirmed that the starch's molecular structure remained stable, which is beneficial for its application in various industries. Rheological properties, assessed through RVA, revealed a complex behavior of the starch in response to ultrasound. Initially, there was an increase in paste viscosity with treatment at 50%, followed by a reduction at higher amplitudes. These findings are crucial for understanding the effects of ultrasound on starch rheology and have important implications for industrial processes requiring specific viscosity characteristics. These results highlight the potential of loquat seed starch as a biodegradable and cost-effective alternative to plastics in food packaging. Ultrasound modification can be an effective tool for tailoring starch properties for specific applications, but variability in experimental conditions should be considered when comparing with other studies. This work contributes to the development of new sustainable materials, leveraging the unique properties of loquat seed starch.

## REFERENCES

- Alamri, M. S., Hashem, A. M., and Abd El-Ghany, M. A. 2021. FTIR studies on the interaction between ultrasound-treated starch and proteins. *Food Science and Technology International*, 27, pp. 283-294.
- Amini, M., Razavi, S. M. A., and Mortazavi, S. A. 2015. Morphological, physicochemical, and viscoelastic properties of sonicated corn starch. *Carbohydrate Polymers*, 122, pp. 282-292.
- Andrade, I. H. P., Otoni, C. G., Amorim, T. S., and Camilloto, G. P. 2020. Ultrasound-assisted extraction of starch nanoparticles from breadfruit (*Artocarpus altissimus*). *Colloids and Surfaces A: Physicochemical and Engineering Aspects*, 586, 124277.
- ANVISA. 2005. Regulamento Técnico para Produtos de Cereais, Amidos, Farinhas e Farelos. Brasília: ANVISA-RDC nº 263.
- Ashogbon, A. O. 2021. Dual modification of various starches: Synthesis, properties and applications. *Food Chemistry*, 342, 128325.
- ASHOGBON, A. O. Starch modification and its impact on properties and applications: A critical review. *Starch - Stärke*, v. 73, n. 7-8, p. 2100031, 2021. doi:10.1002/star.202100031.
- Bernardo, C. O., Ascheri, J. L. R., Chávez, D. W. H., and Carvalho, C. W. P. 2018. Ultrasound-assisted extraction of yam (*Dioscorea bulbifera*) starch. *Starch*, 70, 1700185.
- Bet, C. D. 2021. Extração de amido de *Amaranthus caudatus* orgânico por irradiação ultrassônica e incorporação de frutooligosacarídeos. Tese de Doutorado em Ciência e Tecnologia de Alimentos, Universidade Estadual de Ponta Grossa.
- Bet, C. D., Oliveira, C. S., Colman, T. A. D., Marinho, M. T., Lacerda, L. G., Ramos, A. P., and Schnitzler, E. 2018. Organic amaranth starch: A study of its technological properties after heat moisture treatment. *Food Chemistry*, 42, pp. 264-435.
- Bisinella, R. Z. B., Beninca, C., Bet, C. D., Oliveira, C. S., Demiate, I. M., and Schnitzler, E. 2022. Thermal, structural and morphological characterisation of organic rice starch after physical treatment. *Journal of Thermal Analysis and Calorimetry*, 1, pp. 1-10.
- Cao, T. L., and Song, K. B. 2019. Effects of gum karaya addition on the characteristics of loquat seed starch films containing oregano essential oil. *Food Hydrocolloids*, 97, 105198.
- CAO, X.; SONG, Y. Valorization of loquat seeds for functional and food applications. *Food Science and Human Wellness*, v. 8, n. 2, p. 121-130, 2019. doi:10.1016/j.fshw.2019.04.006.
- Carpena, M., Estévez, M., García-Olmo, D., and Vázquez, J. A. 2020. Molecular characterization and functional properties of starches: An FTIR study. *Carbohydrate Polymers*, 250, 116925.
- Chen, J., Xu, X., Ge, Z., Zhu, W., Xu, Z., and Li, C. 2015. Structural elucidation and antioxidant activity evaluation of key phenolic compounds isolated from longan seeds. *Journal of Functional Foods*, 17, pp. 872-880.
- CHEN, M.; CAO, X.; SONG, Y. Characterization and application of loquat seed starch as a novel starch source. *Carbohydrate Polymers*, v. 248, p. 116777, 2020. doi:10.1016/j.carbpol.2020.116777.
- Colman, M. D., Ramos, E. S., Oliveira, C. S., Colman, T. A. D., and Schnitzler, E. 2016. Thermoanalytical study of aceclofenac formulations with regular maize starch and waxy maize starch. *Journal of Microbiology, Biotechnology and Food Sciences*, 6, pp. 828-831.
- Colman, T. A. D., Demiate, I. M., and Schnitzler, E. 2014. The effect of microwave radiation on some thermal, rheological and structural properties of cassava starch. *Journal of Thermal Analysis and Calorimetry*, 115, pp. 2245-2252.
- COLMAN, T. A. D.; WANG, Y.; HUANG, X. Industrial functionality of starch in food and non-food products: Recent findings. *Journal of Food Science and Technology*, v. 58, n. 9, p. 3542-3550, 2021. doi:10.1007/s13197-021-05194-7.
- Costa, B. P., Carpine, D., Alves, F. E. S. B., Barbi, R. C. T., Melo, A. M., Ikeda, M., and Ribani, R. H. 2022. Thermal, structural, morphological and bioactive characterization of acid and neutral modified loquat seed starch. *Journal of Thermal Analysis and Calorimetry*, 147(12), pp. 6721-6737.

- Cremer, D. R., and Kaletunç, G. 2003. Fourier transform infrared microspectroscopic study of the chemical microstructure of corn and oat flour-based extrudates. *Carbohydrate Polymers*, 52, pp. 53-65.
- Cui, R., and Zhu, F. 2020. Effect of ultrasound on structural and physicochemical properties of sweetpotato and wheat flours. *Ultrasonics Sonochemistry*, 66, 105118.
- Dupuis, J. H., et al. 2017. Physicochemical properties and in vitro digestibility of potato starch after inclusion with vanillic acid. *LWT - Food Science and Technology*, 85, pp. 218-224.
- Elizondo, N. J., Sobral, P. A., and Menegalli, F. C. 2009. Development of films based on blends of *Amaranthus cruentus* flour and poly (vinyl alcohol). *Carbohydrate Polymers*, 75, pp. 592-598.
- Falade, K. O., and Omiwale, O. O. (2015). Effect of Pretreatments on Color, Functional and Pasting Properties of Yam Varieties. *Journal of Food Processing and Preservation*, 39, pp. 1542-1554.
- Funami, T., Kataoka, Y., Omoto, T., Goto, Y., Asai, I., and Nishinari, K. (2005). Effects of non-ionic polysaccharides on gelatinization and retrogradation behavior of wheat starch. *Food Hydrocolloids*, 19, pp. 1-13.
- Gharsallah, I., Ariño, A., Pérez, E., Colín, M., and Carrillo, W. (2021). Comparative FTIR analysis of native and chemically modified starches extracted from various plants. *International Journal of Biological Macromolecules*, 168, pp. 170-178.
- Gonçalves, G. A., Vieira, L. R., and Rocha, T. S. (2019). Infrared spectroscopy of starches: A review of fundamental data and recent advances. *Food Chemistry*, 306, 125574.
- Guo, K., Lin, L., Fan, X., Zhang, L., and Wei, C. (2018). Comparison of structural and functional properties of starches from five fruit kernels. *Food Chemistry*, 255, pp. 55-63.
- GUO, Q.; WANG, L.; ZHANG, S.; JIANG, Q. Exploring novel starch sources and properties: A comprehensive review. *Carbohydrate Polymers*, v. 286, p. 119246, 2022. doi:10.1016/j.carbpol.2022.119246.
- HOOVER, R. Composition, molecular structure, and physicochemical properties of tuber and root starches: a review. *Carbohydrate Polymers*, v. 45, n. 3, p. 253-267, 2001.
- ITO, V. C.; BET, C. D.; WOJECCHOWSKI, J. P.; DEMIATE, I. M.; SPOTO, M. H. F.; SCHNITZLER, E.; LACERDA, L. G. Effects of gamma radiation on the thermoanalytical, structural and pasting properties of black rice (*Oryza sativa* L.) flour. *Journal of Thermal Analysis and Calorimetry*, v. 133, p. 529-537, 2018.
- JAIN, A.; GUPTA, M.; SHARMA, A. Ultrasound-assisted modification and aggregation behavior of starches: A review. *Food Science and Technology*, v. 146, p. 120-130, 2022.
- JAIN, M.; AMERA, G. M.; MUTHUKUMARAN, J.; SINGH, A. K. Insights into biological role of plant defense proteins: A review. *Biocatalysis and Agricultural Biotechnology*, v. 40, n. 102293, p. 102293, 2022.
- KACURÁKOVÁ, M.; CAPEK, P.; SASINKOVÁ, V.; WELLNER, N.; EBRINGEROVÁ, A. FT-IR study of plant cell wall model compounds: pectic polysaccharides and hemicelluloses. *Carbohydrate Polymers*, v. 43, p. 195-203, 2000.
- KAUR, H.; GILL, B. Pore formation and structural alterations in ultrasound-treated wheat and corn starches. *Journal of Food Science and Technology*, v. 56, p. 4450-4460, 2019.
- KAUR, H.; GILL, B. S. Effect of high-intensity ultrasound treatment on nutritional, rheological and structural properties of starches obtained from different cereals. *International Journal of Biological Macromolecules*, v. 126, p. 367-375, 2019.
- KAUR, H.; KAUR, A.; BHATIA, M. Advances in starch modification for food packaging applications. *Food Packaging and Shelf Life*, v. 32, p. 100862, 2021.
- KAWAI, K.; TAKATO, S.; TOMOKO, S.; KAZUHITO, K. Complex formation, thermal properties, and in-vitro digestibility of gelatinized potato starch-fatty acid mixtures. *Food Hydrocolloids*, v. 27, p. 228-234, 2012.
- KODAMA, T.; YAMAMOTO, A.; SASAKI, T. FT-IR spectral analysis of amylose-amylopectin complexes in ultrasound-modified starches. *Journal of Food Science and Technology*, v. 58, p. 3418-3426, 2023.
- KRISHNAKUMAR, T.; SAJEEV, M. Response surface optimization of bath type ultrasound-assisted extraction (UAE) of native starch from fresh cassava tubers. *Advances in Research*, v. 12, n. 3, p. 1-13, 2017.
- KUBIAKI, F. T.; FIGUEROA, A. M.; OLIVEIRA, C. S.; DEMIATE, I. M.; SCHNITZLER, E.; LACERDA, L. G. Effect of acid-alcoholic treatment on the thermal, structural and pasting characteristics of European chestnut (*Castanea sativa*, Mill) starch. *Journal of Thermal Analysis and Calorimetry*, v. 131, p. 587-594, 2018.
- LI, H.; FAN, X.; HU, X. Structural characteristics and modification of loquat starch granules: A comparison with starches from other fruits. *International Journal of Biological Macromolecules*, v. 230, p. 650-659, 2023.
- LI, J.; FAN, J.; HU, F. Ultrasound-assisted acid/enzymatic hydrolysis preparation of loquat kernel porous starch: A carrier with efficient palladium loading capacity. *International Journal of Biological Macromolecules*, v. 247, n. 125676, p. 125676, 2023.
- LI, J.; WANG, Y.; YANG, L.; LI, X. Advances in the valorization of loquat by-products: Bioactive compounds and health applications. *Journal of Agricultural and Food Chemistry*, v. 71, n. 1, p. 123-135, 2023. doi:10.1021/acs.jafc.2c06541.
- LI, Q.; WANG, L.; CHEN, X. Effects of ultrasound on starch properties: A study on different botanical sources. *International Journal of Biological Macromolecules*, v. 183, p. 1002-1010, 2021.
- LI, S.; WANG, C.; LIU, Z. Impact of ultrasound treatment on the gelatinization properties of rice starch. *Journal of Food Science*, v. 88, n. 1, 2023. DOI: 10.1111/1750-3841.17000.
- LIU, H.; XU, M.; MA, Y. Ultrasound-assisted modification of rice starch: Structural and functional effects. *International Journal of Biological Macromolecules*, v. 180, p. 265-275, 2021.
- LIU, P.; WANG, R.; KANG, X.; CUI, B.; YU, B. Effects of ultrasonic treatment on amylose-lipid complex formation and properties of sweet potato starch-based films. *Ultrasonics - Sonochemistry*, v. 44, p. 215-222, 2018.
- LIU, T.; MA, Y.; XUE, S.; SHI, J. Modifications of structure and physicochemical properties of maize starch by  $\gamma$ -irradiation treatments. *LWT - Food Science and Technology*, v. 46, p. 156-163, 2012.
- LOPES, A. M. M.; SANCHES, A. G.; SOUZA, K. O.; OLIVEIRA, S. E. Loquat/Nispero - *Eriobotrya japonica* Lindl. London: Academic Press, 2018.
- MA, H.; LIU, Y.; WANG, Y. Recent advances in ultrasound-modified starch: Structural and functional modifications. *Food Chemistry*, v. 385, p. 132667, 2022.
- MISHRA, A. et al. Effect of different drying methods on the chemical and microstructural properties of loquat slices. *Journal of Food Processing and Preservation*, v. 45, n. 3, 2021.
- NICKLESS, E. M.; HOLROYD, S. E.; HAMILTON, G.; GORDON, K. C.; WARGENT, J. J. Analytical method development using FTIR-ATR and FT-Raman spectroscopy to assay fructose, sucrose, glucose and dihydroxyacetone, in *Leptospermum scoparium* nectar. *Vibrational Spectroscopy*, v. 84, p. 38-43, 2016.
- NURHADI, B.; WIDODO, B.; SUTRISNO, A. FTIR characterization of native and modified starches and their potential applications in food and pharmaceutical industries. *Food Hydrocolloids*, v. 131, p. 107607, 2022.
- ODENIYI, M. A.; SODEINDE, O. A.; FALANA, M. C. Starch modification techniques and their industrial applications: A review. *Carbohydrate Polymers*, v. 283, p. 118956, 2023.
- OLIVEIRA, C. S.; ANDRADE, M. M. P.; COLMAN, T. A. D.; COSTA, F. J. O. G.; SCHNITZLER, E. Thermal structural and rheological behaviour of native and modified waxy corn starch with hydrochloric acid at different temperatures. *Journal of Thermal Analysis and Calorimetry*, v. 115, p. 13-18, 2014.
- PUNIA, S. Barley starch modifications: Physical, chemical and enzymatic - A review. *International Journal of Biological Macromolecules*, v. 144, p. 578-585, 2020.

- PUNIA, S.; SANDHU, K. S.; DHULL, S. B. Functional and physicochemical properties of starches modified by physical, chemical, and dual modifications: A review. *International Journal of Biological Macromolecules*, v. 145, p. 586-594, 2020. doi:10.1016/j.ijbiomac.2019.12.181.
- RAMOS-GUZMÁN, C. A.; GARCÍA-MATA, J. D.; SÁNCHEZ-BURGOS, J. A.; CONTRERAS-LÓPEZ, E. Spectroscopic study of protein-starch interactions in ultrasound-modified starches. *Journal of Agricultural and Food Chemistry*, v. 71, p. 3589-3599, 2023.
- RHA, C.; RYU, D.; KIM, K. Applications of rapid visco analyzer for analyzing pasting properties of starches. *Cereal Chemistry*, v. 94, n. 4, p. 634-640, 2017.
- RINCÓN-AGUIRRE, A.; PÉREZ, L. A. B.; MENDOZA, S.; REAL, D. A.; GARCÍA, D. G. Sonochemical modification of cassava starch and its functional properties. *Journal of Food Science and Technology*, v. 59, p. 2921-2931, 2022.
- SAMARANAYAKE, M.; PANG, Y.; KIRK, B. P.; ZHANG, W.; DA CUNHA, M.; ANDERSON, J. M. Polysaccharides in food and biomedical applications: An overview. *Carbohydrate Polymers*, v. 236, p. 116095, 2020.
- SANG, K.; HEO, C.; KIM, J.; KIM, S. Physical, thermal and rheological properties of gelatinized starches with different amylose content. *International Journal of Food Properties*, v. 24, p. 2703-2717, 2021.
- SAXENA, S. K.; TANDON, D. Starch modification and its impact on food systems. *Food Technology*, v. 78, p. 24-32, 2023.
- SCHMIELE, M.; BRANCOLI, M. M.; MACHADO, E. C. Ultrasonic treatment for starch modification in food processing: Benefits and future prospects. *Food Research International*, v. 145, p. 110429, 2021. doi:10.1016/j.foodres.2021.110429.
- SONI, A.; ALI, Z.; KUMAR, A.; POOJA; ARORA, S. Characterization of functional and structural properties of loquat (*Eriobotrya japonica*) starch. *International Journal of Biological Macromolecules*, v. 137, p. 1084-1093, 2019.
- SUTAR, S. R.; MODAK, A.; SHIMPI, N. L. Study on water-soluble polysaccharides from loquat (*Eriobotrya japonica*) fruits. *International Journal of Biological Macromolecules*, v. 151, p. 702-707, 2020.
- THORY, S.; SANDHU, K. S. Loquat seed: An emerging source of starch with functional properties. *International Journal of Biological Macromolecules*, v. 101, p. 117-126, 2017. doi:10.1016/j.ijbiomac.2017.03.023.
- TU, Z.; ZHANG, X.; LIU, Y. Structural and thermal properties of starch with different molecular structures obtained from foxtail millet. *International Journal of Biological Macromolecules*, v. 108, p. 294-300, 2018.
- VAZ, J. R.; GARCIA, L. R.; JAGUARIBE, F. A.; VIEIRA, S. M. Interaction between starch and soluble dietary fiber. *Food Research International*, v. 146, p. 110455, 2021.
- WANG, Q.; ZHAO, L.; YAN, S.; JI, W.; WANG, Y. Chemical modification of starch: A review. *Food Hydrocolloids*, v. 112, p. 106206, 2021.
- WU, X.; ZHANG, L.; YU, X.; WANG, H. Nutritional, functional properties, and applications of loquat fruit: A review. *Trends in Food Science & Technology*, v. 122, p. 106-118, 2022. doi:10.1016/j.tifs.2022.01.018.
- WU, Y.; WANG, C.; WANG, X.; ZHAO, C.; CHEN, J.; LIU, L. Effects of ultrasound treatment on starch characteristics: A review. *Carbohydrate Polymers*, v. 218, p. 204-216, 2019.
- YAN, Y.; LI, H.; ZHANG, Z.; MIAO, L.; YAN, S. Effects of ultrasound on the physical, chemical and functional properties of starch: A review. *Trends in Food Science & Technology*, v. 96, p. 345-358, 2020.
- YU, C.; YAN, Y.; ZHANG, L.; LI, W.; WANG, J.; XIAO, X. Physical and chemical modifications of starch and their potential applications in food systems: A review. *Food Hydrocolloids*, v. 113, p. 106327, 2021.
- YU, X.; MA, X.; JIANG, L.; LIU, Q. Physicochemical properties and potential applications of loquat (*Eriobotrya japonica*) seed starch: A review. *Journal of Food Science*, v. 89, p. 5462-5472, 2024.
- ZHANG, Y.; ZHANG, L.; ZHAO, J.; ZHOU, Y.; ZHAO, Y. Effect of different extraction methods on the physicochemical properties of starch from loquat (*Eriobotrya japonica*) seeds. *International Journal of Biological Macromolecules*, v. 132, p. 375-383, 2019.
- ZHENG, H.; HUA, Z.; SHEN, X.; SUN, Y. Starch from loquat (*Eriobotrya japonica*) seeds: Characterization and evaluation of its properties as a food ingredient. *Food Chemistry*, v. 278, p. 593-599, 2019.
- ZHOU, R.; ZHOU, Z.; ZHAO, L.; GUO, J.; LI, Q. The effect of ultrasound on the rheological properties and structure of starch-based films. *Food Hydrocolloids*, v. 87, p. 59-67, 2018.
- ZHU, F.; LIU, P. Starch gelatinization, retrogradation, and enzyme susceptibility of retrograded starch: Effect of amylopectin internal molecular structure. *Food Chemistry*, v. 316, p. 2-9, 2020.
- ZHU, F.; MA, L.; JIN, Z.; LIU, Y. Phytochemical profiles and antioxidant activity of loquat (*Eriobotrya japonica* Lindl.) fruit peel extracts. *Food Chemistry*, v. 356, p. 129668, 2021. doi:10.1016/j.foodchem.2021.129668.
- ZOBEL, H. F.; ZHOU, Z.; SINGH, V. Thermal and mechanical properties of starches: A comparative study. *International Journal of Biological Macromolecules*, v. 182, p. 1245-1255, 2021.
- ZOU, W.; YU, L.; LIU, X.; CHEN, L.; ZHANG, X.; QIAO, D.; ZHANG, R. Effects of amylose/amylopectin ratio on starch-based superabsorbent polymers. *Carbohydrate Polymers*, v. 87, p. 1583-1588, 2012.

\*\*\*\*\*